# Grazer behavior can regulate large-scale patterns of community states

Vadim A. Karatayev, Marissa L. Baskett, David J. Kushner, Nicholas T. Shears, Jennifer E. Caselle, Carl Boettiger.

## Abstract

Ecosystem patterning can frequently arise from either environmental heterogeneity or biological feedbacks that produce multiple persistent ecological states. One such possible feedback is density dependent changes in behavior that regulates species interactions, which raises the question of whether behavior can also affect large-scale community patterns. On temperate rocky reefs, kelp and urchin barrens can form mosaics if urchins locally avoid predators and physical abrasion in kelp stands or large-scale patches when starvation intensifies grazing across entire reefs at low kelp density. By fitting dynamical models to large-scale surveys, we find that these behavioral feedbacks best explain observed spatial patterning. In our best-supported models reef-scale feedbacks create reef-scale, alternatively stable kelp- and urchin-dominated states at 37% of reefs in California. In New Zealand, local feedbacks limit this phenomenon to 3-8m depths with moderate wave stress on kelp, with distinct single stable states in exposed shallows and sheltered, deeper areas. Our results highlight that differences in grazer behavior can explain ecosystem patterning.

## Introduction

Spatial patterning in community types characterizes many ecosystems. For example, in arid ecosystems patches of shrubs and barren, dry soil 25 m in diameter form mosaic patterns (Rietkerk & Van de Koppel 2008). On mountain ranges, stripes of ribbon forests 200-500m wide intersperse with wider bands of grassy meadows. In lakes, turbid-water states with high algal densities dominate fertilized lake basins 5-10km long while less polluted basins remain in a clear-water state characterized by aquatic vegetation (van den Berg et al. 1998). A longstanding focus of empirical and theoretical work has aimed to resolve the processes generating ecosystem patterns and their spatial scale.

Spatial patterning may occur due to underlying environmental heterogeneity or, in homogeneous abiotic environments, arise from local biotic feedbacks. Examples of environment-driven patterns include gradients in wave stress that zone seaweed communities from wave-tolerant to more sensitive species with increasing water depth (Shears & Babcock 2004) and localized disturbances such as lightning-induced fires that create meadow patches within forests. In homogeneous environments self-organized patterns arise when biological feedbacks reinforce distinct ecological states. If interactions change from positive to negative with distance, mosaics of populated and empty areas occur. For example, in arid ecosystems mosaics arise because shrubs collect water from the surrounding soil and alpine ribbon forests form as trees displace growth-inhibiting snow into adjacent grassy areas (Rietkerk & Van de Koppel 2008). If feedbacks are independent of distance, they can interact with environmental heterogeneity to drive patterns over large scales. For instance, grasses pre-

dominate in areas of low-moderate herbivory by dissipating grazing across many individuals but collapse to a low-density state from overgrazing in areas with high livestock densities (Noy-Meir 1975). In either case, feedback-induced patterning requires strong and often non-linear species interactions.

One driver of interaction strength are density-dependent changes in behavior. In predator-prey systems, abundant prey can reduce predation by sharing social information within and across prey species (Gil *et al.* 2018). Likewise, predator presence can discourage herbivory in dense plant aggregations, for instance in Yellowstone National Park where wolf re-introduction allowed aspen recovery near forest edges (Laundré *et al.* 2001). Behavioral avoidance of predators can reduce herbivory by 90% (trout and mayflies, McPeek and Pekarsky 1998), whereas herbivore activity as part of large groups that reduce predation risk can account for a majority of total consumption (68%, fish on coral reefs, Gil and Hein 2017). Increased foraging rates can also arise as resource declines cause starvation (Harrold & Reed 1985). This potential for density to feed back and affect biotic interactions through behavior raises the question of whether behavior can also affect large-scale community patterns.

Temperate rocky reefs exemplify each of patterned communities, behavior-mediated herbivory, and environmental variation. Patterning of two distinct ecological states, kelp forests and urchin-dominated barrens (Fig. 1a, b), can occur in these ecosystems at drastically different scales in different regions. Large-scale ($>$ 1km) barrens and forests spanning all depths characterize California reefs while in New Zealand kelp occupy deeper water and urchins shallower areas in smaller-scale ($<$ 100 m) bands. This difference might arise from a greater sensitivity of the dominant kelp species in New Zealand to wave stress, which peaks at shallower depths, compared to the canopy-forming dominant kelp species in California. Alternatively, these regions may differ in the roles of behavioral feedbacks controlling urchin grazing activity, which might intensify in local patches where kelp densities are insufficient to physically deter urchins (Konar 2000) in New Zealand. In California, grazing can instead increase synchronously across the reef when low kelp densities lead to insufficient subsidies of kelp fronds drifting to urchins sheltering on the seafloor (Ebeling *et al.* 1985; Harrold & Reed 1985). Resolving whether biotic feedbacks and distinct states can explain temperate reef spatial patterning can also provide insight into the scientific debate on whether or not urchin barrens and kelp forests occur as alternative stable states (Petraitis & Dudgeon 2004).

We resolve how environment, urchin densities, and urchin behavior drive kelp densities by comparing how well dynamical models incorporating each feature can explain field data. For this we develop a general, model of kelp population dynamics on temperate reefs and synthesize data across large-scale surveys in California and New Zealand. We then analyze our best-fitting models to resolve the spatial patterns and potential for community-wide alternative stable states in each system.

# Methods

## 2.1 Study systems

We focus our analysis on temperate rocky reefs in Northeast New Zealand (NZ) and the California Northern Channel Islands (CA) dominated by kelp (*Macrocystis pyrifera*, CA, and *Eklonia radiata*, NZ) or urchins (*Evechinus chloroticus* in NZ and *Strongylocentrotus purpuratus, S. franciscanus* in CA). Like many temperate reefs, high rates of kelp growth and urchin grazing characterize these systems: abundant urchins can denude kelp forests in weeks, while under low urchin densities kelp can recolonize barrens within a few months (Ebeling *et al.* 1985). By contrast, the abundance of comparatively longer-lived urchins (5-50 years) changes more slowly in response to urchin predator abundance and multi-year changes in ocean climate (Shears et al. 2013; Okamoto 2014). This difference in time scales means that kelp reach steady state abundance under a given urchin density, whereas urchin density is largely independent of kelp abundance because urchin populations are demographically open (Okamoto 2014) and can maintain high densities in the absence of kelp (Filbee-Dexter & Scheibling 2014; Ling *et al.* 2015).

Urchin grazing activity can strongly decline with either local- or reef-scale kelp density. Urchins typically remain in rock crevices that offer refuge from storms and predators, consuming only kelp fronds detached from plants by waves and carried to the bottom by currents over 100-1000m ('drift kelp' hereafter; Ebeling *et al.* 1985; Harrold & Reed 1985). When this long-distance subsidy becomes insufficient at low kelp and high urchin densities, urchins across the reef synchronously emerge from refugia to actively graze on kelp. More locally, dense stands of kelp can physically abrase urchins as plants move with waves (Konar 2000) and can shelter urchin predators that lead to cryptic behavior (Cowen 1983); both mechanisms reduce urchin grazing activity. Density-dependent consumption present in both reef- and local-scale feedbacks can theoretically create alternative stable states with either high or low resource abundance (Bate & Hilker 2014).

## 2.2 Data

We use survey data sampling 200-300km coastlines in each region, with 71 reefs sampled in 2001 in Northeast New Zealand (Shears & Babcock 2004) and 93 reefs sampled over 5-30 years in the California Channel Islands (Kushner *et al.* 2013; PISCO *et al.* 2011). This geographic extent spans a wide range of environmental conditions and urchin densities, allowing us to independently estimate the effects of each model process. This spatial scale also makes our findings robust to inter-annual variation in the primary environmental drivers (e.g., storms, temperature, upwelling) because these factors are autocorrelated at smaller spatial scales in both systems (10-50km; Cavanaugh *et al.* 2013). Additionally, availability of long-term data at California reefs (10 years at each reef on average) allows us to verify our assumption that kelp reach steady states within a single year (see "Role of behavioral feedbacks" below). Samples in both systems were collected at the end of the growing season, when kelp reach peak abundance levels (July-August in CA, March-June in NZ).

Samples in each system span c.a. $500m^2$ of each reef. The environmental drivers we

account for are total urchin predator density (2 species in NZ, 3 species in CA), wave stress based on wind fetch (NZ) or year-specific maximum wave height (CA), light penetration in the water (i.e., visibility), and nitrate concentrations derived from water temperature (CA only; Bell *et al.* 2018). Each reef was sampled using transects with 15-50 1-5m$^2$ quadrat samples that span a 2-20m water depth gradient, translating to 1,273 samples in NZ and 14,955 samples in CA. Data collected in each quadrat include densities of adult kelp and urchins of sufficient size to consume kelp (>25mm test diameter), sample location along transect, and depth. Given that water depth attenuates both wave stress and light, we adjust these estimates to the depth of each sample. For this we use the standard relations of light extinction and dissipation of wave energy (Bekkby *et al.* 2008), adjusted for regional differences in wave dissipation using a fitted parameter (see 'Model description' below).

To compare the spatial extent of kelp- and urchin-dominated regimes in New Zealand and California, we categorize the community state in each sample (Fig. 1a, b). Given that low urchin densities can maintain barren regimes, we classify samples containing urchins and few kelp ($< 0.05$ ind $m^{-2}$ in CA, $< 0.5$ ind $m^{-2}$ in NZ) as urchin-dominated; we classified all other samples as kelp-dominated. We then calculate the scale of patterning (Fig. 1c, d) as the distance at which Pearson correlation in community state $\kappa$, calculated over a 5km window moving by 0.5km, declines to zero (with standard error $\sqrt{(1-\kappa^2)/(n-2)^{-1}}$ given $n$ comparisons).

## 2.3 Model description

Our model follows dynamics of local (1-5m$^2$) adult kelp abundance $N_q$ (Fig. 2), with dynamics across locations on each reef potentially coupled by kelp dispersal and urchin behavioral feedbacks. Kelp $N_q$ reproduce continuously during the year with a baseline per capita fecundity $r$. In California, fecundity can decline due to limitation of nitrate $G$ that arises at high water temperatures; we model this dependence using a function that saturates to 1 at high nitrate levels, $g(G) = G(1 + vG)^{-1}$. Newly produced spores can disperse over short distances ($< 500m$ for *Macrocystis*, Anderson and North 1966, Reed et al. 1992). Therefore, we model the density of spores arriving in a location $q$ as a combination of (1) the fraction $\gamma$ of all spores dispersing across the reef $s$ given kelp density averaged over the reef, $N_s = k^{-1} \sum_{q=1}^{k} N_q$, and (2) the fraction $1 - \gamma$ of locally produced spores dispersing $< 5m$.

Survival of settled juvenile kelp to adult stages depends on both local and reef-scale factors. To model light limitation of juveniles by competitively dominant adults, we assume that light availability declines proportionally with adult density $N_q$ from the baseline light availability on the reef $L_s$. Due to their greater palatability compared with adults, juveniles also experience high rates of grazing $\delta_J$, which may depend on urchin behavior (described below). On the reef scale, we account for environmentally-driven stochasticity in survival (e.g., as might be due to thermal stress or interspecific competition) using a log-normally distributed random variable $S_R$ with a mean of one and standard deviation $\sigma$, with $S_R$ realizations identical across all locations in each reef. Finally, given fast maturation (1-2 mo.) and high sensitivity of juveniles to competition and grazing, we model recruitment as a process happening continuously throughout the year.

Adult kelp experience mortality due to wave stress $E$ and grazing by urchins $\delta_A$, which may additionally depend on urchin behavioral feedbacks. Following Bekkby *et al.* 2008 we model reduced wave stress dissipation at more exposed sites. This relation depends on region-specific oceanographic features, here approximated by the parameter $f_w$. For both juvenile and adult kelp mortality from grazing, we assume that urchin density $U$ is constant on the time scale of annual kelp dynamics but grazing rate can dynamically depend on adult kelp density. To model high grazing at moderate kelp densities and low grazing at high kelp densities, we use an inverse-quadratic decline in grazing with kelp density and a per-kelp grazing inhibition factor $\xi_A$. This 'Type IV' functional response represents emergent prey or resource defense (Koen-Alonso 2007; Bate & Hilker 2014), and in our model depends on either $N_q$ for the local-scale feedback or average kelp density across the reef ($N_s$) in reef-scale feedbacks. To account for the possibility that high kelp densities might not completely prevent grazing, we let a fraction of grazing activity depend on behavior, with $1 - f_b$ independent of behavior. Altogether, the behavior-mediated decline in urchin grazing is

$$b(N) = 1 - f_b + \frac{f_b}{1 - (\xi_A N)^2}. \tag{1}$$

The overall dynamics of local kelp abundance are then

$$\frac{dN_q}{dt} = rg(G)(\gamma N_s + (1-\gamma)N_q)\frac{\sigma_R(L - dN_q)}{1 + \delta_R U b(N_x)} - \mu E \exp(f_w E^{-1})N_q - \delta_A U b(N_x) N_q, \tag{2}$$

where $N_x = N_q$ for the local-scale behavior feedback and $N_x = N_s$ for the reef-scale feedback.

## 2.4 Model analyses

To compare the role of each potential driver (environmental, urchin density, behavioral), we compare the fit of both the full model (Eqn. 2) and simpler models with one or two of these processes. This allows us to resolve the independent and interactive effects of drivers; we also include a model with density dependence only as a baseline reference of model performance. Given that fast-growing kelp populations can quickly adjust to changes in abiotic conditions and urchin densities (see "Study system" above), we assume that observed annual kelp densities are at that year's steady-state and compare them with equilibria of fitted models. We tested this assumption by checking that the best-fitting parameter estimates in all models converge to steady state within one year. Additionally, this approach assumes independence of kelp densities among years, which may be less likely when extreme disturbances severely deplete kelp populations across large spatial scales.

We fit models to data using a maximum likelihood approach that accounts for model mis-specification and observation errors. To account for mis-specification that occurs through juvenile survival stochasticity $S_R$, we run each model under 30 values of $S_R$. We solve each model using a Runge-Kutta method in R 3.4.3 (R Core Team 2017), with kelp density initialized at the 5th and 80th percentiles of observed densities in order to resolve the potential presence of alternative stable states. We then compare predicted local kelp densities with observed kelp counts in quadrats using a Poisson likelihood that accounts for observational

Table 1: Model parameters and covariates. Covariates are given by environmental data and parameters are estimated in model fitting. Covariates without units are proportions of region-specific maximum values.

| **Parameter** | **Units** | **Description** |
|---|---|---|
| $r$ | $\mathrm{yr}^{-1}$ | Adult kelp fecundity |
| $v$ | | Half-saturation constant of nitrate in fecundity |
| $\sigma_R$ | | Lognormal model mis-specification in recruit survival |
| $\gamma$ | | Fraction of kelp spores dispersing across reef |
| $d$ | $\mathrm{N}^{-1}$ | Kelp competition for light inhibiting recruitment |
| $\mu$ | $\mathrm{yr}^{-1}$ | Kelp mortality from wave stress |
| $f_w$ | $\mathrm{m}^{-1}$ | Per-meter wave energy dissipation |
| $\delta_A$ | $\mathrm{U}^{-1}\mathrm{yr}^{-1}$ | Max grazing intensity on adult kelp |
| $\delta_R$ | $\mathrm{U}^{-1}$ | Max grazing intensity on kelp recruits |
| $f_b$ | | Fraction of grazing activity affected by behavior |
| $\xi_A$ | $\mathrm{N}^{-1}$ | Inhibition of grazing by kelp |
| **Covariate** | **Units** | **Description** |
| $Z$ | m | Sample depth |
| $L$ | | Local (depth-dependent) light availability |
| $U$ | | Local urchin density |
| $E$ | | Reef-scale wave stress |
| $G$ | | Reef-scale nitrate availability (CA only) |
| $P$ | ind $\mathrm{m}^{-2}$ | Reef-scale urchin predator density |

errors. Averaging likelihood across the 60 simulations in each sample and summing the likelihood across all samples in each region, we arrive at the total likelihood of each model under a given parameter set. Note that in California we evaluate model fit to data collected across all years, although in preliminary analyses we found analogous results limiting the analysis to only a single sampling year from each reef.

For each model, we find the set of best-fitting parameters using the DIRECT global optimization algorithm (Jones et al. 1993) in the package nloptr (Johnson 2019). We then compare model performance using the Akaike Information Criterion (AIC), where AIC difference of $> 4$ suggests improved model fit (Bolker 2008), and also calculate the correlation between predicted and observed kelp presence for a more intuitive reference of model fit.

Using the best-fitting models from each region, we project predicted community patterns across levels of grazing and wave stress. To resolve the effect of grazing we simulate 40 reefs with reef-scale urchin densities spanning the range of values observed in each system. Given that wave stress predominantly depends on water depth rather than reef-scale characteristics, at each reef we additionally simulate 30 locations spanning the range of depths in data. Throughout, we set urchin distribution across depths and reef-scale exposure, light availability, and predator density to the average values observed in data. We compare model

projections with observed kelp patterns smoothed using 2-d splines in the mgcv package.

For each region we also use the best-fitting models with behavior to evaluate the role of alternative stable states in explaining observed patterns. For this we quantify how model performance corresponds to the predicted frequency of alternative stable states across all samples. To control the frequency of alternative stable states, we fix grazing inhibition by kelp $\xi_A$, the parameter controlling feedback strength, at levels increasing from 0 (i.e., no alternative stable states possible in model) to 25% above the best-fit estimate of $\xi_A$. For each $\xi_A$ level, we then optimize all other parameters to determine the best possible model performance and the corresponding frequency of alternative stable states. To evaluate the potential for alternative stable states that span entire reefs specifically, we examine how steady-state kelp presence, averaged across all depths, depends on initial kelp abundance. We examine this dependence across levels of reef-wide urchin density, which can depend on reef-scale management efforts that regulate fishing intensity on urchin predators or urchin harvest (Hamilton and Caselle 2015; House 2017). For reference, we compare predictions from our best-fitting models both with and without the behavioral feedbacks, and also with the reef-scale average frequency of kelp- and urchin-dominated regimes as determined in Figure 1a, b.

# Results

## 3.1 Role of urchin behavior

Behavior-mediated grazing in California and an interactive effect of behavior-mediated grazing and environmental variation in New Zealand predominantly explain patterns in field data (Table 2). Best-fitting models in both regions include environment, grazing, and behavior, and explain a substantial fraction of variation in kelp occurrence across all samples ($R^2 = 0.30$ in NZ and 0.54 in CA). In California, models with grazing and behavioral feedbacks alone outperform models with only grazing and environment (2577 AIC difference). This contrasts New Zealand, where models with environment alone better explain the data than models with only grazing and behavior ($\Delta$ AIC=12); however, a model incorporating all three processes greatly outperforms all other models ($\Delta$ AIC $\geq$ 176). In both regions, models with behavior outperform models without behavior because they can explain the co-occurrence of high and low kelp densities at intermediate urchin densities (Fig. 4). Identical model ranking and comparable parameter estimates also arise in temporally explicit model fits in California, despite the stronger temporal variation in abiotic conditions and urchin densities in this region. In models with behavior, local-scale grazing feedbacks in New Zealand and reef-scale grazing feedbacks in California best explain the data (Table 2).

## 3.2 Drivers of community patterning

The local scale of behavioral feedbacks and a decline in wave stress with depth together explain the much smaller scale of community patterning in New Zealand than in California. In New Zealand, our best-fitting model predicts barrens as the only stable state in shallow areas ($< 3m$) due to a combination of grazing and high wave stress (Fig. 3). At greater water

depths that largely attenuate waves ($> 8m$), we predict forests are the only stable state because kelp quickly form dense stands that inhibit grazing. At intermediate wave stress between these zones, we predict that alternative stable states spanning 1-5m$^2$ patches arise as urchins largely avoid grazing in dense kelp stands and graze intensively elsewhere. This interface occurs at greater depths and urchin barrens cover a larger fraction of the system on reefs with greater overall urchin densities. In California, we predict that community regimes simultaneously span all reef depths due to the weaker role of wave stress and the larger scale of grazing feedbacks (Table 2).

### 3.3 Presence of alternative stable states

Our best-fitting models predict that alternative stable states occur locally in both regions (40% of CA samples, 18% of NZ samples, Fig. 3, 4), but alternative stable states at the scale of entire reefs only in California (Fig. 5). In New Zealand, our best-fitting model predicts that final reef state depends little on initial kelp abundance because alternative stable states occur over only a narrow range of depth-dependent wave stress intensities.

## Discussion

### 4.1 Behavioral feedbacks as drivers of patterning

Our results show that behavior can determine the presence and scale of community patterning by mediating consumer-resource interactions in rocky temperate reefs. This potential occurs through feedbacks where density-dependent changes in behavior amplify consumption when resources decline. In heterogeneous environments, the scale of this feedback determines the spatial extent of the resulting resource- or consumer-dominated community regimes. Specifically, we find that forests and barrens spanning entire reefs in California are most consistent with large-scale feedbacks, where drift kelp are transported over large distances and starvation-induced active grazing occurs when kelp densities decline across entire reefs (Table 2; Harrold & Reed 1985). By contrast, in New Zealand localized feedbacks involving short-distance grazing deterrence by kelp (Konar 2000) can explain fine-scale patterning of community regimes organized into distinct depth zonation by a gradient in wave stress.

In many systems, analogous behavior-induced community patterning may be more likely to arise from resource group defense than consumer starvation. Starvation-induced active urchin grazing can create persistent patterns because, after overgrazing kelp, urchins can survive for decades with little food due to low metabolic costs (Filbee-Dexter & Scheibling 2014; Ling *et al.* 2015). In homeothermic taxa or in warmer systems, prolonged starvation can cause mortality or emigration, allowing eventual resource recovery. High starvation mortality or movement potential at low resource density can therefore lead to long-term consumer-resource cycles, which may additionally propagate across space as grazing fronts in systems where consumers can move freely (Silliman et al. 2013). Conversely, persistent patterns of sparse and abundant prey or plants can arise when dense resources exhibit group defense or modify local environments (e.g., by attracting predators), thereby shifting predation or herbivory to less defended species or to locations where resources are sparse (Schneider and

Kefi 2016).

Behavioral feedbacks may also be more likely to pattern communities in conjunction with co-occurring feedback processes or under stronger environmental heterogeneity. High resource abundance can reduce per-capita mortality through a dilution effect in many systems where consumer density predominantly depends on conditions during critical periods or life stages rather than on resource abundance. Strong dilution feedbacks can produce alternatively stable consumer- or resource-dominated states that span individual pastures (Noy-Meir 1975), coral reefs (Mumby *et al.* 2007), and lakes (Downing et al. 2012). However, co-occurring behavior and dilution feedbacks can also produce patch-scale alternative stable states synergistically even when individually each feedback is insufficient to do so (van de Leemput *et al.* 2016). Finally, feedbacks too weak to drive alternative stable states under the same conditions can still produce distinctive shifts in ecological states over a narrow range of environments ('phase shifts', Scheffer *et al.* 2009). In this case, behavior can transform gradual spatial variation in long-term environmental conditions into relatively distinct ecological states.

## 4.2 Detection of alternative stable states

Behavioral feedbacks drive patchy spatial patterning in our best-supported models by giving rise to alternative stable states. Therefore, our results support the relevance of this phenomenon across both regions, especially in California given the greater frequency of samples with alternative stable states (37% *versus* 15% in NZ, Table 2). This difference in predicted prevalence of alternative stable states is partly due to the regional differences in feedback scale, with more local feedbacks in New Zealand limiting alternative stable states to reef depths with intermediate wave stress on kelp (Fig. 3). These localized states average out to produce a gradual reef-wide response to changes in urchin density and little-no dependence of reef state on initial kelp abundance in New Zealand, while large-scale feedbacks in California produce alternative stable states spanning entire reefs (Fig. 5). This result supports existing theory predicting that relevance of alternative stable states requires either spatially homogeneous environments or a high mobility of matter or organisms involved in ecological feedbacks (van Nes & Scheffer 2005).

Our analysis also represents a novel approach to quantify empirical support for alternative stable states. Preceding studies based on mechanistic models detect this phenomenon by fitting model dynamics to time series (e.g., Ives *et al.* 2008). However, such analyses remain rare because long-term monitoring data is available for only a few systems thought to exhibit alternative stable states. Instead, we fit model steady states to spatial survey data by utilizing time scale differences between behavior and kelp abundance and the comparatively slow, longer-term changes in urchin abundance and the environment. Our approach compensates for limited time series by leveraging spatial replication of data across gradients in 'slower' variables and yields model ranking and parameter estimates analogous to conventional time series model fitting.

## 4.3 Community patterning on temperate rocky reefs

Our results suggest that the spatial scale of ecological feedbacks can explain the scale of spatial patterning across temperate rocky reefs. High levels of drift kelp that likely underlie reef-scale behavioral feedbacks in California also occur in Chile, where the dominant urchin relies predominantly on passive grazing (Vásquez *et al.* 1984). Feedbacks in kelp-urchin interactions might also underlie large-scale forests and barrens when kelp facilitate recruitment of urchin predators that freely forage across entire reefs (Smith & Herrkind 1992; Karatayev and Baskett 2019). Our results highlight how behavior might strengthen this feedback by resolving declines in grazing activity with predator density in both regions, complementing analogous findings in California (Ebeling *et al.* 1985; Caselle *et al.* 2018). Conversely, the ubiquity of depth gradients in wave stress suggests a limited potential for reef-scale forests and barrens to arise from feedbacks involving local processes. This may include feedbacks where kelp physically deter grazing ('whiplash'), hinder urchin movement, or reduce survival of urchin larvae compared to barren areas. Our model predictions in New Zealand indicate that such local feedbacks may however explain the distinctive, mosaic boundaries between kelp- and urchin-dominated areas frequently observed locally on temperate rocky reefs (Vásquez & Buschmann 1997).

The potential for alternative stable states to pattern an ecosystem at region-specific scales found here can also help explain the debated presence of alternative stable states on temperate reefs. Empirically resolving the presence of this phenomenon remains difficult because experimental manipulations and measurements of ecological feedbacks are typically constrained to small temporal and spatial scales (Petraitis and Dudgeon 2004). To date alternative stable states are best associated with California and Alaska reefs, where disturbances induce persistent and large-scale barrens, but remain debated in other regions despite the global prevalence of kelp- and urchin-dominated states (Ling *et al.* 2015; Filbee-Dexter & Scheibling 2014). Our results suggest that this debate may arise because the spatial scale of alternative stable states can be highly region-specific. This reflects existing empirical work resolving how the spatial scale of this phenomenon determines the patchiness scale in arid systems (Kefi et al. 2007), mudflats (van de Koppel et al. 2008), and the rocky intertidal (Petraitis 2013). Given these findings, we emphasize that future studies and syntheses estimate the potential scale of alternative stable states by quantifying the smallest observed areas of each state or the spatial scale of underlying ecological feedbacks.

## 4.4 Results robustness

To avoid model over-fitting, our approach leaves out additional potential dynamics that might drive alternative stable states and therefore patchy spatial patterning in temperate rocky reefs. First, we do not consider competition among primary producers, which might displace competitively inferior juvenile stages of *Eklonia* and *Macrocystis*. However, few samples in our data indicate competitive exclusion by lacking both kelp and urchins ($< 10\%$; Fig. 1); additionally, our approach might implicitly account for competition with more wave-tolerant species present in shallower areas by over-estimating the direct role of depth-dependent wave stress. Second, our focus on kelp and behavioral dynamics ignores longer-term feedbacks affecting urchin and urchin predator abundances that can theoretically

drive alternative stable states. These include predator recruitment facilitation by kelp (Smith & Herrkind 1992) and urchin recruitment facilitation by crustose coralline algae present in barrens (Baskett & Salomon 2010); see Ling *et al.* 2015 for a full array of potential feedbacks. Finally, seasonality in kelp wave mortality (predominantly in winter) and recruitment (predominantly in spring) might weaken our assumption that kelp abundance reaches steady state within a year. Such transients can obscure the detection of equilibria (Mumby *et al.* 2013) and cause us to under-estimate the role of alternative stable states.

We also omit several secondary urchin behaviors that can increase the role of behavioral feedbacks in both regions. First, our model tracks urchin grazing activity but ignores local-scale urchin movement in response to kelp density, which in New Zealand might explain higher urchin densities in shallower areas. On some temperate rocky reefs, urchin aggregations in mobile grazing fronts can produce shifts to large barren areas (Silliman *et al.* 2013; Filbee-Dexter & Scheibling 2014). However, the role of kelp in spatial urchin distributions in New Zealand is unclear because barrens do not appear to expand following regular, synchronous kelp declines induced by senescence. Second, we limited model comparison to select a single behavioral feedback that best explains patterns in each region, whereas in reality both deterrence and drift subsidies might influence grazing activity (e.g., AUS drift kelp paper). However, we point out that physical deterrence through whiplash is unlikely among tall, adult giant kelp plants dominant in California; similarly, a much smaller total kelp biomass in New Zealand (0.05 kg $m^{-2}$, Shears & Babcock 2004) compared to California (2 kg $m^{-2}$, Cavanaugh *et al.* 2011) might limit the magnitude of drift subsidies. Finally, available data likely underestimates urchin densities at low grazing activity in California because urchins sheltering in rock crevices are harder to detect; in turn, our model fits might underestimate the role of behavioral feedbacks in limiting urchin grazing in kelp forests.

Figure 1: (a, b) Region-specific distribution of kelp- and urchin-dominated states, delineated by dashed blue lines, with N indicating total numbers of samples. (c, d) Spatial scales of correlation in community state (defined as kelp presence). Red points in (c) indicate mean correlation; lines in (d) denote mean correlation ±99% confidence intervals.

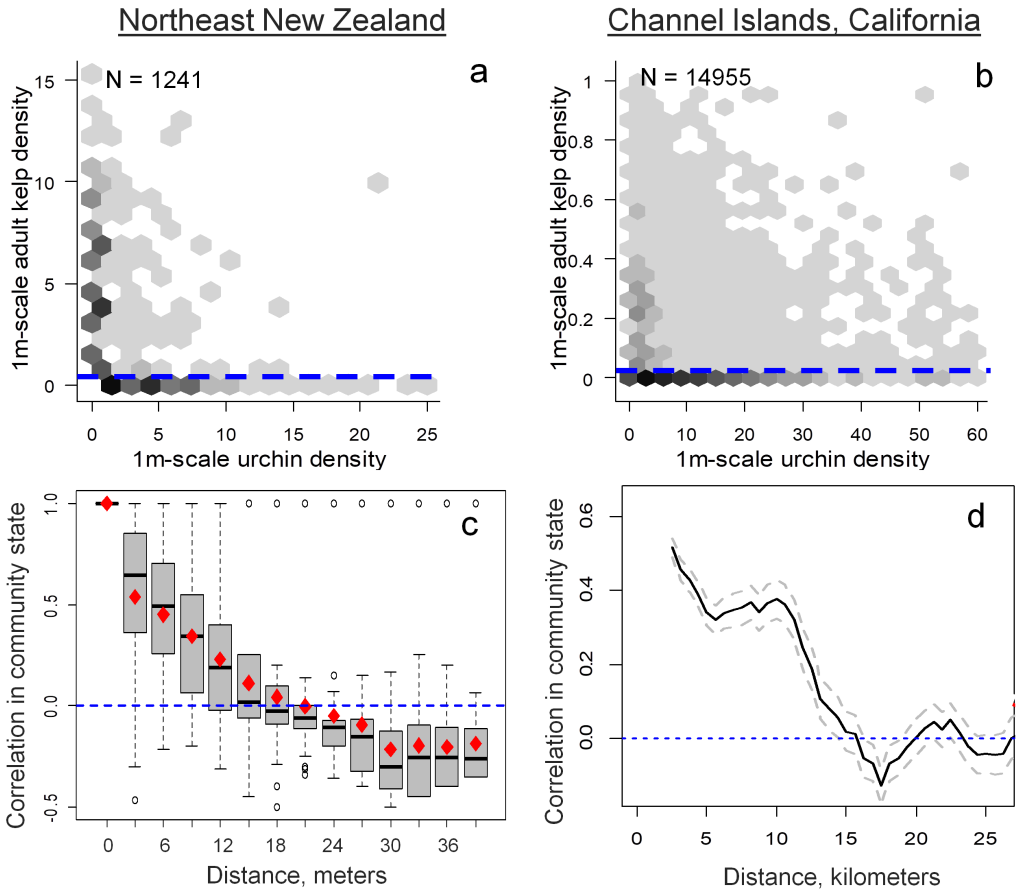

Figure 2: Model layout. (a) Local samples (red rectangles) on each reef span a depth gradient controlling wave intensity. Across reefs, forested and barren community types follow depth zonation in New Zealand but span entire reefs in California. (b) Dynamics of local kelp abundance $N_q$ depend on factors affecting adult survival (red lines), recruitment (black lines), and urchin behavior (blue lines). Circular endpoints on lines denote negative effects and arrows denote positive effects. (c) Functional form of behavioral feedbacks (left), wherein urchins graze less at high kelp density due to either high levels of passive drift kelp subsidies (reef-scale feedbacks, right) or deterrence by predators and physical abrasion in kelp stands (local feedbacks, bottom right).

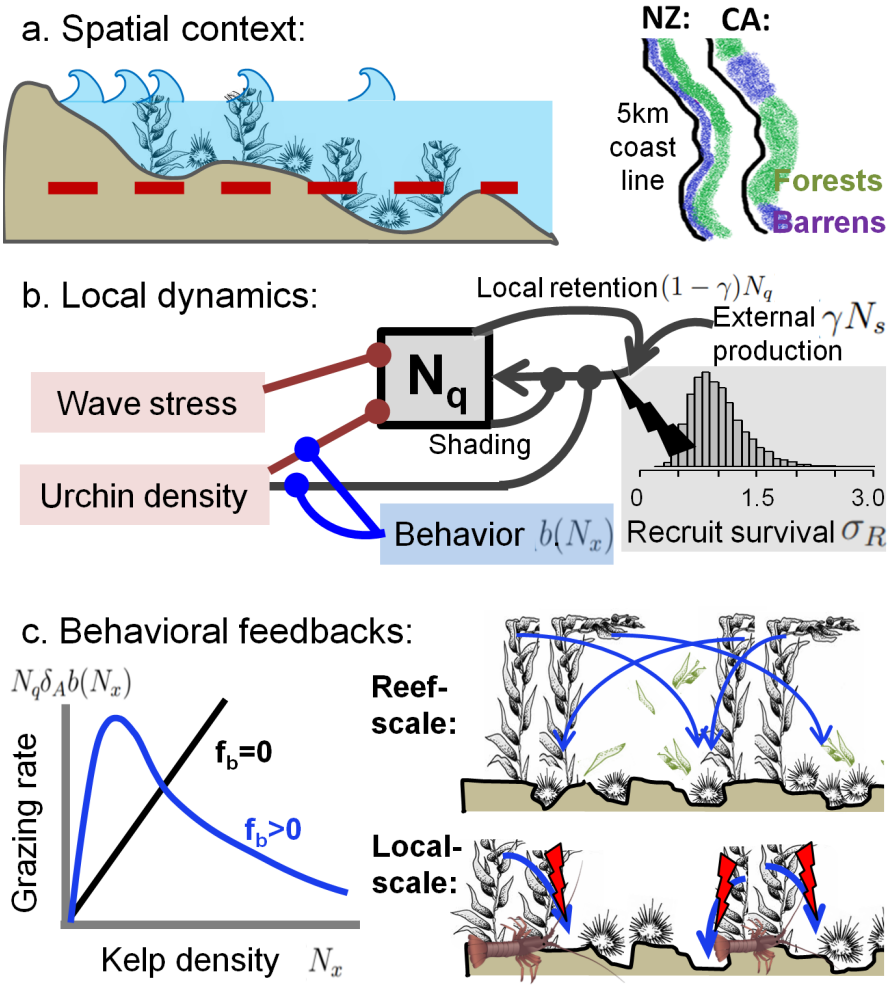

Figure 3: Best-fitting models with behavioral feedbacks reproduce patterns of kelp abundance (colors) in both regions. (a, c) Patterns in observed kelp density across depths on each reef (y-axes) and across reefs with increasing average urchin density. (b, d) Kelp densities predicted by best-fitting models in each region, with secondary y-axes denoting the best-fit, depth-dependent estimates of mortality induced by wave stress. Gray dots in (a, c) denote the sample coverage across these conditions. Hashed boxes in (b, d) denote conditions for which best-fitting models predict alternative stable states with kelp present or absent.

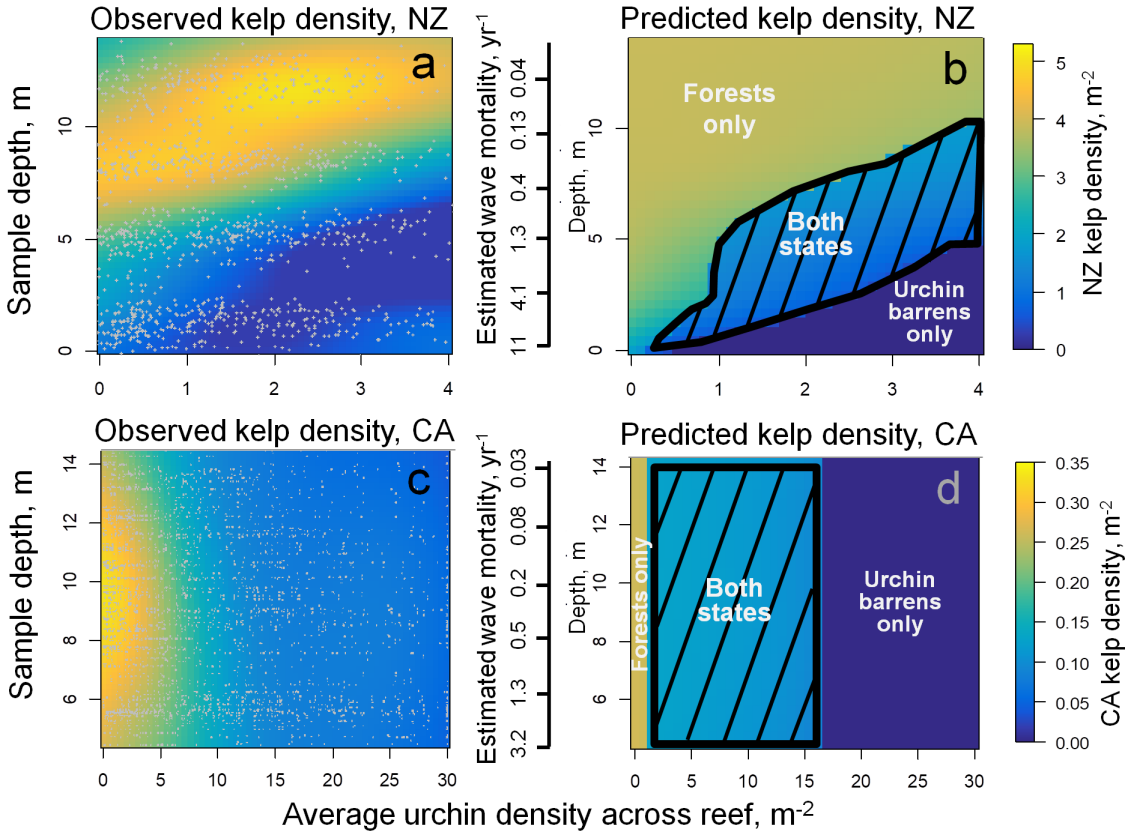

Figure 4: Behavioral feedbacks best explain observed patterns by predicting alternatively stable kelp- and urchin-dominated states. (a, b) Kelp density predicted by best-fitting models without behavior (gray lines) and models with behavior (black lines) for simulations with initially high (solid lines) and initially low kelp densities (dashed lines; without behavior, identical to the solid line). Blue lines in (a, b) denote the average difference in log likelihood between models with and without behavior, with positive differences denoting better fit. (c, d) Performance of models with behavior in each region (black lines) and the fraction of all samples for which models predict alternative stable states (blue lines). Note the comparison of local kelp densities in (a) and reef-scale kelp densities in (b), reflecting the region-specific scale of feedbacks in our best-fitting models (Table 2).

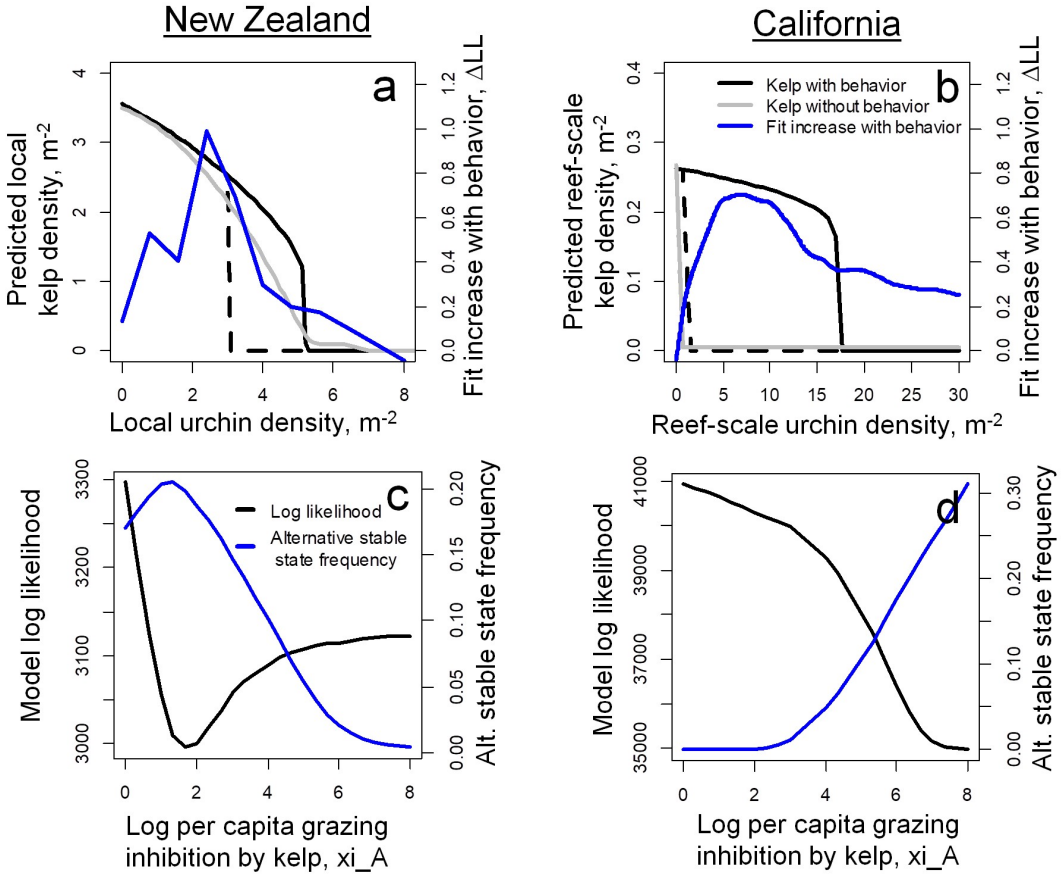

Figure 5: Best-fitting models with behavioral feedbacks predict a relevance of reef-wide alternative stable states with increasing reef-scale urchin densities in California (b) but not in New Zealand (a). (a, b) Frequency of kelp presence across reef predicted by best-fitting models without behavior (red lines) and models with behavior (black lines) for simulations with initially high (solid lines) and initially low kelp densities (dashed lines, not visible without behavior). Blue dots show frequencies of kelp presence across all samples on each reef, with different dots representing different reefs and (in d) reefs in different years.

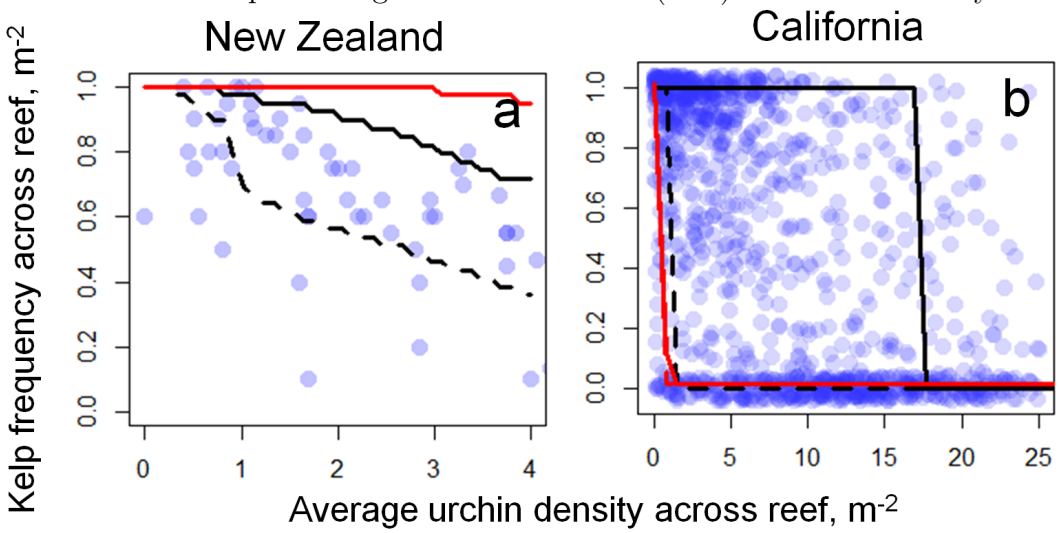

Table 2: Results of model fitting and model comparison in New Zealand (top half) and California (bottom half). Capital letters denote models including environment (E), urchin grazing (U), urchin behavior (B), or density dependence only (DD, present in all models). Subscripts further denote whether behavior includes predator avoidance (P), local-scale feedbacks (Local), or reef-scale feedbacks (Reef). pA.S.S. denotes the proportion of observations for which each model predicts alternative stable states.

| Model | $r$ | $\sigma_R$ | $\gamma$ | $d$ | $\mu$ | $\delta_A$ | $\delta_R$ | $f_b$ | $\xi_A$ | $\xi_P$ | AIC | ΔAIC | pA.S.S. |
|---|---|---|---|---|---|---|---|---|---|---|---|---|---|
| E,U,B$_{Local,P}$ | 18.0 | 0.34 | 0 | 0.4 | 2.65 | 1.53 | 4.79 | 0.97 | 1.94 | 9.65 | 2899 | 0 | 0.24 |
| E,U,B$_{Reef,P}$ | 16.0 | 0.34 | 0 | 0.5 | 2.66 | 2.45 | 4.18 | 0.84 | 48.9 | 11.0 | 3075 | 176 | 0.00 |
| E,U | 19.1 | 0.34 | 0 | 0.5 | 0.88 | 0.75 | 1.78 | | | | 3394 | 496 | 0 |
| E | 14.0 | 0.14 | 0 | 0.3 | 2.66 | | | | | | 3423 | 525 | 0 |
| U,B$_{Local}$ | 16.9 | 0.34 | 0 | 0.3 | | 1.40 | 4.51 | 0.85 | 52.7 | | 3435 | 536 | 0.12 |
| U | 19.5 | 0.34 | 0 | 0.3 | | 0.48 | 2.35 | | | | 3508 | 609 | 0 |
| U,B$_P$ | 19.5 | 0.34 | 0 | 0.3 | | 0.51 | 2.29 | | | 10.8 | 3511 | 613 | 0 |
| U,B$_{Reef}$ | 18.0 | 0.34 | 0 | 0.3 | | 1.55 | 2.66 | 0.77 | 85.1 | | 3526 | 627 | 0.00 |
| DD | 18.0 | 0.06 | 0 | 0.4 | | | | | | | 3936 | 1038 | 0 |
| E,U,B$_{Reef,P}$ | 11.0 | 0.34 | 1 | 3.3 | 1.52 | 1.11 | 3.33 | 0.97 | 4160 | 8.66 | 33501 | 0 | 0.24 |
| E,U,B$_{Local,P}$ | 11.0 | 0.34 | 1 | 3.9 | 1.52 | 1.11 | 3.33 | 0.97 | 4160 | 11.7 | 34290 | 789 | 0.20 |
| U,B$_{Local}$ | 18.3 | 0.34 | 1 | 4.5 | | 1.48 | 2.54 | 0.98 | 2109 | | 36386 | 2885 | 0.35 |
| U,B$_{Reef}$ | 10.8 | 0.34 | 1 | 5.2 | | 1.45 | 2.59 | 0.98 | 2538 | | 36952 | 3451 | 0.27 |
| E,U | 12.1 | 0.34 | 1 | 3.9 | 0.78 | 0.37 | 0.37 | | | | 39529 | 6028 | 0 |
| U,B$_P$ | 19.3 | 0.34 | 1 | 4.1 | | 0.48 | 0.75 | | | 11.1 | 41168 | 7667 | 0 |
| U | 19.3 | 0.34 | 1 | 4.1 | | 0.47 | 0.50 | | | | 41186 | 7685 | 0 |
| DD | 2.00 | 0.34 | 1 | 8.3 | | | | | | | 49484 | 15983 | 0 |

# References

Baskett, M.L. & Salomon, A.K. (2010). Recruitment facilitation can drive alternative states on temperate reefs. *Ecology*, 91, 1763–1773.

Bate, A.M. & Hilker, F.M. (2014). Disease in group-defending prey can benefit predators. *Theoretical Ecology*, 7, 87–100.

Bekkby, T., Isachsen, P.E., Isæus, M. & Bakkestuen, V. (2008). Gis modeling of wave exposure at the seabed: a depth-attenuated wave exposure model. *Marine Geodesy*, 31, 117–127.

Bell, T.W., Reed, D.C., Nelson, N.B. & Siegel, D.A. (2018). Regional patterns of physiological condition determine giant kelp net primary production dynamics. *Limnology and Oceanography*, 63, 472–483.

Bolker, B.M. (2008). *Ecological models and data in R.* Princeton University Press.

Caselle, J.E., Davis, K. & Marks, L.M. (2018). Marine management affects the invasion success of a non-native species in a temperate reef system in california, usa. *Ecology Letters*, 21, 43–53.

Cavanaugh, K.C., Kendall, B.E., Siegel, D.A., Reed, D.C., Alberto, F. & Assis, J. (2013). Synchrony in dynamics of giant kelp forests is driven by both local recruitment and regional environmental controls. *Ecology*, 94, 499–509.

Cavanaugh, K.C., Siegel, D.A., Reed, D.C. & Dennison, P.E. (2011). Environmental controls of giant-kelp biomass in the Santa Barbara Channel, California. *Marine Ecology Progress Series*, 429, 1–17.

Cowen, R.K. (1983). The effects of sheephead (*Semicossyphus pulcher*) predation on red sea urchin (*Strongylocentrotus franciscanus*) populations: an experimental analysis. *Oecologia*, 58, 249–255.

Ebeling, A.W., Laur, D.R. & Rowley, R.J. (1985). Severe storm disturbances and reversal of community structure in a southern california kelp forest. *Marine Biology*, 84, 287–294.

Filbee-Dexter, K. & Scheibling, R.E. (2014). Sea urchin barrens as alternative stable states of collapsed kelp ecosystems. *Marine Ecology Progress Series*, 495, 1–25.

Gil, M.A., Hein, A.M., Spiegel, O., Baskett, M.L. & Sih, A. (2018). Social information links individual behavior to population and community dynamics. *Trends in Ecology & Evolution*, 33, 535–548.

Harrold, C. & Reed, D.C. (1985). Food availability, sea urchin grazing, and kelp forest community structure. *Ecology*, 66, 1160–1169.

Ives, A.R., Einarsson, Á., Jansen, V.A.A. & Gardarsson, A. (2008). High-amplitude fluctuations and alternative dynamical states of midges in lake myvatn. *Nature*, 452, 84.

Johnson, S.G. (2019). The nlopt nonlinear-optimization package. URL `http://ab-initio.mit.edu/nlopt`.

Koen-Alonso, M. (2007). A process-oriented approach to the multispecies functional response. In: *From energetics to ecosystems: the dynamics and structure of ecological systems*. Springer, pp. 1–36.

Konar, B. (2000). Seasonal inhibitory effects of marine plants on sea urchins: structuring communities the algal way. *Oecologia*, 125, 208–217.

Kushner, D.J., Rassweiler, A., McLaughlin, J.P. & Lafferty, K.D. (2013). A multi-decade time series of kelp forest community structure at the california channel islands: Ecological archives e094-245. *Ecology*, 94, 2655.

Laundré, J.W., Hernández, L. & Altendorf, K.B. (2001). Wolves, elk, and bison: reestablishing the" landscape of fear" in yellowstone national park, usa. *Canadian Journal of Zoology*, 79, 1401–1409.

Ling, S.D., Scheibling, R.E., Rassweiler, A., Johnson, C.R., Shears, N., Connell, S.D. *et al.* (2015). Global regime shift dynamics of catastrophic sea urchin overgrazing. *Philosophical Transactions of the Royal Society B-Biological Sciences*, 370.

Mumby, P.J., Hastings, A. & Edwards, H.J. (2007). Thresholds and the resilience of caribbean coral reefs. *Nature*, 450, 98–101.

Mumby, P.J., Steneck, R.S. & Hastings, A. (2013). Evidence for and against the existence of alternate attractors on coral reefs. *Oikos*, 122, 481–491.

Noy-Meir, I. (1975). Stability of grazing systems: an application of predator-prey graphs. *Journal of Ecology*, 459–481.

Okamoto, D.K. (2014). *The role of fluctuating food supply on recruitment, survival and population dynamics in the sea*. University of California, Santa Barbara.

Petraitis, P. (2013). Multiple stable states in natural ecosystems. In: *Multiple stable states in natural ecosystems*. Oxford University Press, New York, NY, pp. 1–188.

Petraitis, P.S. & Dudgeon, S.R. (2004). Detection of alternative stable states in marine communities. *Journal of Experimental Marine Biology and Ecology*, 300, 343–371.

PISCO, Carr, M. & Caselle, J. (2011). Pisco: Subtidal: Community surveys: Swath surveys. URL `{http://search.dataone.org/view/doi:10.6085/AA/pisco_subtidal.151.2}`.

R Core Team (2017). R: A language and environment for statistical computing.

Rietkerk, M. & Van de Koppel, J. (2008). Regular pattern formation in real ecosystems. *Trends in Ecology & Evolution*, 23, 169–175.

Scheffer, M., Bascompte, J., Brock, W.A., Brovkin, V., Carpenter, S.R., Dakos, V. *et al.* (2009). Early-warning signals for critical transitions. *Nature*, 461, 53–59.

Shears, N.T. & Babcock, R.C. (2004). *Community composition and structure of shallow subtidal reefs in northeastern New Zealand*. Department of Conservation Wellington.

Silliman, B.R., McCoy, M.W., Angelini, C., Holt, R.D., Griffin, J.N. & van de Koppel, J. (2013). Consumer fronts, global change, and runaway collapse in ecosystems. *Annual Review of Ecology, Evolution, and Systematics*, 44, 503–538.

Smith, K.N. & Herrkind, W.F. (1992). Predation on early juvenile spiny lobsters panulirus argus (*Latreille*): influence of size and shelter. *Journal of Experimental Marine Biology and Ecology*, 157, 3–18.

van de Leemput, I.A., Hughes, T.P., van Nes, E.H. & Scheffer, M. (2016). Multiple feedbacks and the prevalence of alternate stable states on coral reefs. *Coral Reefs*, 35, 857–865.

van Nes, E.H. & Scheffer, M. (2005). Implications of spatial heterogeneity for catastrophic regime shifts in ecosystems. *Ecology*, 86, 1797–1807.

Vásquez, J.A. & Buschmann, A.H. (1997). Herbivore-kelp interactions in chilean subtidal communities: a review. *Revista Chilena de Historia Natural*, 70, 41–52.

Vásquez, J.A., Castilla, J.C. & Santelices, B. (1984). Distributional patterns and diets of four species of sea urchins in giant kelp forest(macrocystis pyrifera) of puerto toro, navarino island, chile. *Marine Ecology Progress Series*, 19, 55–63.